Originally Published in:
IEEE Transactions on Parallel and Distributed Systems
Volume 25, Issue 1
January 2014

Surface Coverage in Sensor Networks

Linghe Kong, Mingchen Zhao, Xiao-Yang Liu,
Jialiang Lu, *Member, IEEE,* Yunhuai Liu, *Member, IEEE,*
Min-You Wu, *Senior Member, IEEE,* Wei Shu, *Senior Member, IEEE,*

Abstract—Coverage is a fundamental problem in Wireless Sensor Networks (WSNs). Conventional studies on this topic focus on 2D ideal plane coverage and 3D full space coverage. The 3D surface of a Field of Interest is complex in many real world applications. However, existing coverage studies do not produce practical results. In this paper, we propose a new coverage model called *surface coverage*. In surface coverage, the Field of Interest is a complex surface in 3D space and sensors can be deployed only on the surface. We show that existing 2D plane coverage is merely a special case of surface coverage. Simulations point out that existing sensor deployment schemes for a 2D plane cannot be directly applied to surface coverage cases. Thus, we target two problems assuming cases of surface coverage to be true. One, under stochastic deployment, what is the expected coverage ratio when a number of sensors are adopted? Two, if sensor deployment can be planned, what is the optimal deployment strategy with guaranteed full coverage with the least number of sensors? We show that the latter problem is NP-complete and propose three approximation algorithms. We further prove that these algorithms have a provable approximation ratio. We also conduct extensive simulations to evaluate the performance of the proposed algorithms.

Index Terms—Wireless Sensor Networks, Surface Coverage, Expected Coverage Ratio, Optimal Coverage Strategy

1 Introduction

Coverage problem is fundamental in Wireless Sensor Networks (WSNs). Each sensor is deployed to sense a section of a Field of Interest (FoI). A FoI is considered fully covered if and only if every point on the surface is covered by at least one sensor. The quintessence of the coverage problem is to use the least number of sensors to satisfy specific service requirements, e.g. coverage ratio, network connectivity and robustness. Solutions to the coverage problem have important applications in base station deployment in cellular networks, coverage in wireless mesh networks, etc.

Existing works on coverage issues focus mainly on 2D plane coverage or 3D full space coverage. In 2D plane coverage [16] [3], sensors are only allowed to be deployed on an ideal plane. And, in 3D full space coverage [10] [26], the FoI is assumed to be the 3D full space where sensors can be positioned freely within the whole FoI.

In many real world applications, however, the FoI is neither a 2D ideal plane nor a 3D full space. Instead, they are complex surfaces. For example, in the Tungurahua volcano monitoring project [1] (Fig.1), sensors are deployed on the volcano, which is a surface. Existing 2D plane coverage solutions do not provide a workable strategy. If the 2D uniform deployment is adopted, there will be some coverage dead zone on the complex surface as illustrated in Fig.2 (we called Coverage Dead Zone Problem). Similarly, 3D full space coverage solutions cannot be applied either, because sensors in this case can only be deployed on the exposed surface area, and not freely inside the volcano or in the air. Three-dimensional full space coverage solutions are not discussed in this paper because they differ fundamentally from issues of complex surface coverage.

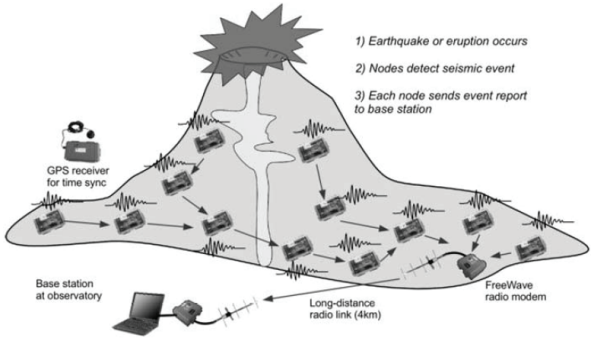

Fig. 1. A case study of the volcano monitoring project by Harvard Sensor Networks Lab [1], which is a typical surface coverage.

In order to address the coverage solution in the surface applications, we propose an innovative model called surface coverage. The surface coverage in WSNs (complex surfaces) is superior to solutions derived from conventional 2D ideal plane and 3D full space coverage methodologies. Nonetheless, the advantages of surface coverage come with new challenges such as how to handle variations in the shape of the surface. This paper studies two problems in WSN surface coverage. One, computing the expected coverage ratio when a given number of sensors are scattered under stochastic deployment. Two, finding the optimal deployment strategy with guaranteed full coverage and the least number of sensors when sensor

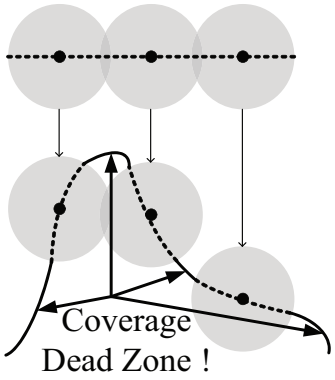

Fig. 2. The coverage dead zone problem occurs when the traditional 2D plane solution 'uniform distribution' is directly adopted on a 3D surface (side view).

deployment is pre-determined. We prove that the optimum surface coverage problem is NP-complete when applied to complex surface. Then, we propose three approximation algorithms with a provable performance bound for coverage of complex surfaces. The methodology used in this paper can be extended to other issues in surface coverage, e.g. connectivity problems and mobility problems.

The main results and contributions are summarized as follows:

- To our best knowledge, this is the first work to tackle the surface coverage problem in WSNs. We propose a new model for the coverage problem.
- We derive analytical expressions of the expected coverage ratio on surface coverage for stochastic deployment. Simulation experiments are conducted to verify the results.
- We formalize the planned deployment problem and prove that it is NP-complete. Three approximation algorithms are proposed with provable approximation performance.
- We build the problem scope of surface coverage, which includes diverse dimensions. We also discuss the availability of our methods in different type of FoIs, sensors, distributions, and other requirements.

The rest of the paper is organized as follows. In Section 2, we summarizes the related works. In Section 3, we discuss the assumptions and models used throughout the paper. In Section 4, we present the analytical results of the expected coverage ratio under stochastic deployment. In Section 5, we describe the solution to the optimum deployment strategy under planned deployment. We evaluate our results in Section 6. We discuss some practical issues in Section 7. Section 8 concludes the paper. In the supplemental material, Section 1 gives the detailed proofs of all theorems in this paper and Section 2 extends our method to other cases in the problem scope.

2 Related Work

2.1 Coverage of the 2D Plane and the 3D Space

There are several ways to classify existing research on the coverage problem. One is the type of FoI: 2D ideal plane FoI [22] [13] [18] [25] [20] [6] [16] [11] [17] [7] [4] [24] [5] [3] or 3D full space FoI [10] [26]. Early work on coverage for the 2D ideal plane assumed that the plane was infinite so as to avoid the edge effect [20] [16] [11] [3], but recent findings have shown these results to be impractical and offer tentative solutions to finite areas [17] [4]. As yet, fundamental problems for these finite areas remain unanswered (e.g. optimum coverage policy and mobile coverage), and coverage solutions for the 2D ideal plane continue to incite heated debate [24] [3]. Still, proposed solutions to the 2D ideal plane problem have found a wide range of applications and some of them are easily applied to the case of 3D full space. All of these results, derived from the 2D plane and then applied to 3D complex surface, suffer from the Coverage Dead Zone Problem.

Another way to classify existing work is by the type of sensors. Some early works assumed that sensors were static and homogeneous. More recent work began to consider mobile sensors [20] [24][15] and heterogeneous sensors [17]. For example, mobile sensors were employed to cover a certain area so that fewer static sensors were needed [20] [24]. Lazos [17] applied a new mathematical tool called "Integral Geometry" to solve the coverage problem when sensors are heterogeneous. Parts of our results are extended from the results from this work [17].

A third way to classify previous research is based on the deployment scheme. A deterministic scheme [11] [3] is a planned deployment (e.g., manual deployment [8]) that needs fewer sensors to cover a given area but is more time-consuming and labor intensive. Another deployment scheme is by stochastic or random deployment, which is advocated in [20] [17] [4] [24]. This method deploys sensors by vehicles or aircraft. We consider both of these cases.

Also, there is other work that focus on joint optimum coverage goals. Cardei et. al. [6] proposed a scheduling policy to maximize the lifetime while covering. Paper [13] studied the relation between sensing coverage and communication connectivity. And in works [11] [3], the optimum coverage patterns for an ideal infinite plane with designated connectivity requirements were proposed. In particular, the recent barrier coverage [16] [7] [4] considered intrusion detection in a barrier area, which is quite different from traditional 2D plane coverage. All these works are, however, based on the 2D ideal plane and no complex surface in 3D space has yet been considered.

TABLE 1
Notations and Terms in Section 3

Symbol	Definition
SP3	Space surface Poisson point process model;
PP3	Planar surface Poisson point process model;
OSCP	The optimum surface coverage problem;
S	The bounded area of the 3D surface;
P	A set of points (positions in S) to deploy sensors;
$g^*(P)$	The union set of the coverage area if sensors are deployed at P;
C	A feasible solution of P meets OSCP.

2.2 Coverage of the 3D Surface

Currently, several works started to study the surface coverage problem.

A distributed algorithm [27] was proposed to produce a triangulation for any arbitrary 2D and 3D sensor networks. Further, [12] studied the optimal solution for 3D surface sensor deployment with minimized overall unreliability. It also designed a series of excellent algorithms for practical implementation. This study focused on the homogeneous sensors with the deterministic deployment.

Liu et. al. [21] derived the expected coverage ratios for regular terrains by cone/cos model and for irregular terrains by digital elevation model. This work assumed that homogeneous sensors are stochastically deployed.

Compared with the recent works, in our paper, we build the problem scope of surface coverage, which includes different type of FoIs, sensors, distributions, and other requirements. Our analysis methods and algorithms could be extended to these various dimensions.

3 Problem Statement

In this section, the problem scope of surface coverage is described. Then, sensor, surface and distribution models are formulated. This is followed by a formal statement of the surface coverage problem in WSNs. And a brief summary of integral geometry and the Poisson point process are presented.

3.1 Problem Scope

The problem scope of surface coverage can be divided into several dimensions.

• The type of FoI: (i) The FoI is a bounded (finite) surface in 3D space. (ii) The FoI has or has no hole on the surface.

• The type of sensors: (i) The sensors are static or mobile. (ii) The sensing areas of all sensors are homogeneous or heterogeneous.

• The type of sensor distribution: deterministic deployment or stochastic deployment.

• The coverage requirement: (i) full coverage or multiple coverage. (ii) coverage with or without the consideration of connectivity.

Throughout the main parts of this paper, we study the case that the FoI is a finite surface in 3D space without hole, the sensors are static and their sensing areas are homogeneous, both deterministic and stochastic deployment are studied, and the requirement is full coverage without connectivity limitation. In Section 2 of the supplemental document, we extend our method to other cases in the problem scope.

3.2 Sensor models

We assume that all sensors have the same sensing radius r in 3D Euclid space. They are statically deployed and stationary after deployment. A point is said to be *covered* by a sensor if it is located within the sensing area of the sensor. The FoI is thus partitioned into two regions: the *covered region*, which is covered by at least one sensor and the *uncovered region*, which is the complement of the covered region.

3.3 Surface models

The surface can be expressed as $z = f(x, y)$ in a Cartesian coordinate system, which is considered the *reference system* for this surface. We assume that the FoI is convex, i.e., $z = f(x, y)$ is a single valued function. A surface is a *plane* if and only if the function is $z = c$ where c is a constant. A surface is a *slant* if and only if the function is $z = ax + by + c$ where a, b, c are constants. A sensor is said to be placed on the surface if its position lies on the surface. In this paper, we consider the FoI to be finite for practice. Thus, the boundary effect will be taken into account in all our calculations.

3.4 Sensor distribution models

Definition 3.1. *The* Z-projection *of a point in 3D space is its projection point along the Z axis on the xOy plane in the reference system, i.e., if the Cartesian coordinates of a point is (x, y, z), the coordinates of its projection is $(x, y, 0)$. The* Z-projection *of a set in 3D space is a planar point set in xOy plane, which contains all the Z-projection points in the set.*

For stochastic deployment, we consider two sensor distribution models. One is the *space surface Poisson point process model (SP3)* and the other is the *planar surface Poisson point process model (PP3)*.

- SP3 is described as $p_m = \frac{(\rho F)^m}{m!} e^{-\rho F}$.
- PP3 is described as $p_m = \frac{(\rho F')^m}{m!} e^{-\rho F'}$.

Where p_m is the probability that there are exactly m sensors on a FoI, where F is the area of the surface FoI, and F' is the Z-projection area of the FoI. It can be seen that both models agree with the traditional distribution model (i.e. Poisson Point Process) when the surface is an ideal plane.

Fig.3 illustrates the difference between SP3 and PP3 models from a side view. SP3 model is used

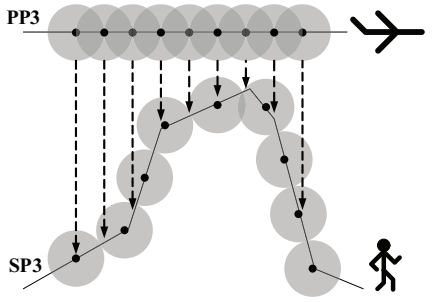

Fig. 3. The difference between PP3 and SP3 models.

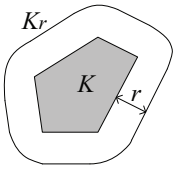

Fig. 4. An example of a parallel convex set.

to describe that sensors are deployed by humans or vehicles running on the surface. Hence, the sensors follow the Poisson distribution according to the surface. PP3 model is used to describe that sensors are deployed by aircraft. The scattered sensors follow the Poisson distribution according to the flight path. Fig.3 shows a typical example: 9 sensor nodes (SP3) are isometric according to the surface, while thee nodes (PP3) are isometric according to the flight line. When the nodes (PP3) drop along with the arrows, the deployed positions by two models are different.

3.5 Problem statements

Definition 3.2. *Let $z = f(x, y)$ be a surface S in 3D space. Let $\parallel S \parallel$ be the area of the surface S. The function $g : S \rightarrow 2^S$ is a function defined on the surface. Its value is the point set which is covered by sensor when the independent variable is the position of the sensor. The function $g^* : 2^S \rightarrow 2^S$ is a set function defined as: $C \subseteq S$, $g^*(C) = \bigcup_{t \in C} g(t)$.*

Simply, the function $g(P)$ describes the coverage area of a sensor if it is deployed at position P on the surface, when P has only one point. $g^*(P)$ presents the union set of the coverage area of sensors if they are deployed at positions P, when P is a set of points.

Definition 3.3. The coverage ratio *is defined as: Given a point set $P(P \subseteq S)$, the coverage ratio f_c is a real value expressed as*

$$f_c = \frac{\parallel g^*(P) \parallel}{\parallel S \parallel}. \tag{1}$$

Because f_c depends on the deployment of sensors P, we focus on the expected value of the coverage ratio $E(f_c)$ when P follows some distribution.

Definition 3.4. *A feasible solution to the coverage problem is defined as a point set C that satisfies $C \subseteq S, g^*(C) \supseteq S$.* The optimum surface coverage problem (OSCP) *is defined as: $minimize|C|, C$ is a feasible solution.*

3.6 Integral geometry and Poisson Point Process

Lemma 3.1. *The Z-projection of a convex set $\mathcal{C}$ in 3D space is a planar convex set.*

Definition 3.5. *Parallel convex sets. The parallel set K_r, in the distance r of a convex set K is the union of all closed circular disks of radius r, the centers of which are points of K. The boundary ∂K_r, is called the outer parallel curve of ∂K in the distance r.*

Fig.4 gives an example of a parallel convex set.

Lemma 3.2. *Let the area of the convex set K be F and perimeter of the convex set be L. Then the area F_r and perimeter L_r of the parallel convex set K_r is:*

$$F_r = F + Lr + \pi r^2 \tag{2}$$

$$L_r = L + 2\pi r \tag{3}$$

Definition 3.6. *Poisson Point Process. Let $\mathcal{D}_0$, $\mathcal{D}$ be two domains of the plane such that $\mathcal{D} \subseteq \mathcal{D}_0$. Let F_0, F be the areas of $\mathcal{D}_0$, $\mathcal{D}$. According to the density $dP = dx \wedge dy$, the probability that a random point of $\mathcal{D}_0$ lies in D is F/F_0. If there are n points chosen at random in $\mathcal{D}_0$, the probability that exactly m of them lie in $\mathcal{D}$ is a* binomial distribution

$$p_m = \binom{n}{m} \left(\frac{F}{F_0}\right)^m \left(1 - \frac{F}{F_0}\right)^{n-m} \tag{4}$$

If $\mathcal{D}_0$ expands to the whole plane and both n, $F_0 \rightarrow \infty$ in such a way that $\frac{n}{F_0} \rightarrow \rho$, which is a positive constant, we get

$$\lim p_m = \frac{(\rho F)^m}{m!} e^{-\rho F} \tag{5}$$

The right-hand side of Eqn. 5 is the probability function of the Poisson distribution*; it depends only on the product ρF, which is called the parameter of the distribution. This probability model for points in the plane is said to be a* homogeneous planar Poisson point process of intensity *ρ. In the following, we simplify it as* Poisson Point Process*.*

Lemma 3.3. *Let $\mathcal{A}_0$ be a fixed convex set of area F_0 and perimeter L_0, and let $\mathcal{A}_1$ be a convex set of area F_1 and perimeter L_1. $\mathcal{A}_1$ is randomly dropped in the plane in such a way that it intersects with $\mathcal{A}_0$. The probability that a randomly selected point $P \in \mathcal{A}_0$ is covered by $\mathcal{A}_1$ is given by:*

$$p(P \in \mathcal{A}_1) = \frac{2\pi F_1}{2\pi(F_0 + F_1) + L_0 L_1} \tag{6}$$

Lemma 3.4. *Let $\mathcal{A}_0$ and $\mathcal{A}_1$ be two fixed convex set of area F_0, F_1 and perimeter L_0, L_1, and $\mathcal{A}_0 \subseteq \mathcal{A}_1$. Let $\mathcal{A}_2$ be a convex set of area F_2 and perimeter L_2, randomly dropped*

TABLE 2
Notations and Terms in Section 4

Symbol	Definition
$\mathcal{A}_f$	A field of interest (FoI);
F_f	The area of $\mathcal{A}_f$;
L_f	The perimeter of $\mathcal{A}_f$;
$\mathcal{A}_s$	A sensor;
r	The sensing range of a sensor;
$E(f_c)$	The expected coverage ratio;
θ	The angle between the slant and the xOy plane;
p	The probability.

in the plane in such a way that it intersects with $\mathcal{A}_1$. The probability that it intersects with $\mathcal{A}_0$ is given by:

$$p(\mathcal{A}_0 \bigcap \mathcal{A}_2 \neq \emptyset \mid \mathcal{A}_1 \bigcap \mathcal{A}_2 \neq \emptyset) = \frac{2\pi(F_0+F_2)+L_0L_2}{2\pi(F_1+F_2)+L_1L_2} \tag{7}$$

For more detailed proofs of Lemma 3.1, 3.2, 3.3, and 3.4, please refer to the book [23].

4 Expected Coverage Ratio under Stochastic Distribution Models

4.1 Expected coverage ratio on a plane

Theorem 4.1. *Let $\mathcal{A}_f$ be a FoI of area F_f and perimeter L_f on a plane, and let every sensor $\mathcal{A}_s$ have the same sensing radius r. N sensors are stochastically placed on the plane in such a way that it intersects with $\mathcal{A}_f$ according to PP3 model or SP3 model. The expected coverage ratio $E(f_c)$ of the FoI $\mathcal{A}_f$ is given by:*

$$1-\left(1-\frac{2\pi^2r^2}{2\pi\left(\pi r^2+F_f\right)+2\pi rL_f}\right)^N \tag{8}$$

Proof: Please refer to the supplemental document for the detailed proof of Theorem 4.1. □

Corollary 4.1. *Let $\mathcal{A}_f$ be a FoI of area F_f and perimeter L_f on a plane. Let the distribution of the sensors with sensing radius r be PP3 model or SP3 model with intensity λ. The expected coverage ratio $E(f_c)$ of the FoI $\mathcal{A}_f$ is:*

$$1-\left(1-\frac{2\pi^2r^2}{2\pi\left(\pi r^2+F_f\right)+2\pi rL_f}\right)^{\lambda\left(F_f+L_fr+\pi r^2\right)} \tag{9}$$

Proof: Please refer to the supplemental document for the detailed proof of Corollary 4.1. □

4.2 Expected coverage ratio on a slant

Theorem 4.2. *Let $\mathcal{A}_f$ be a FoI of area F_f and perimeter L_f on a slant. Let the distribution of the sensors with sensing radius r be SP3 model with intensity λ. The expected coverage ratio $E(f_c)$ of the FoI $\mathcal{A}_f$ is:*

$$1-\left(1-\frac{2\pi^2r^2}{2\pi\left(\pi r^2+F_f\right)+2\pi rL_f}\right)^{\lambda\left(F_f+L_fr+\pi r^2\right)} \tag{10}$$

Proof: Please refer to the supplemental document for the detailed proof of Theorem 4.2. □

Lemma 4.1. *For any slant in reference system, if its included angle with the xOy plane is θ, the ratio between the area of any convex area and its Z-projection convex area is a constant. Its value equals to $\sec\theta$.*

Lemma 4.1 can be immediately obtained from trigonometric function.

Theorem 4.3. *Let $\mathcal{A}_f$ be a FoI of area F_f and perimeter L_f on a slant whose equation can be expressed as $z = ax+by+c$. Let the distribution of the sensors with sensing radius r be PP3 model with intensity λ. The expected coverage ratio $E(f_c)$ of the FoI $\mathcal{A}_f$ is:*

$$1-\left(1-\frac{2\pi^2r^2}{2\pi\left(\pi r^2+F_f\right)+2\pi rL_f}\right)^{\lambda\cos\theta\left(F_f+L_fr+\pi r^2\right)} \tag{11}$$

where

$$\theta=\arccos\left(\frac{1}{\sqrt{a^2+b^2+1}}\right) \qquad 0\le\theta<\frac{\pi}{2} \tag{12}$$

Proof: Please refer to the supplemental document for the detailed proof of Theorem 4.3. □

4.3 Results for general complex surface

We simplify the complex surface into many small triangles as many small slants. From this, we are able to obtain an approximate value for the coverage ratio when sensors are stochastically deployed. Let $\mathcal{A}_f$ be the FoI with area F_f and perimeter L_f. We divide $\mathcal{A}_f$ into many small pieces of triangle $\mathcal{A}_i$, with area F_i and perimeter L_i, where i varies from 1 to n. We model the sensing area of the sensor as a sphere with radius r. Let $\mathcal{A}_s$ be the sensing region of the sensor with area $F_s=\pi r^2$ and perimeter $L_s=2\pi r$. In this paper, we assume that the variations in the surface are not significant within the sensing area of a single sensor. As mentioned, we discuss two sensor distribution models separately.

Theorem 4.4. *(for space surface Poisson Point Process model (SP3)) Let the sensor distribution be SP3 on a general complex surface. The probability that a randomly chosen point P in $\mathcal{A}_f$ is covered by the sensor is given by:*

$$p(P\in\mathcal{A}_s)=\frac{2\pi^2r^2}{2\pi\left(\pi r^2+F_f\right)+2\pi rL_f} \tag{13}$$

Proof: Please refer to the supplemental document for the detailed proof of Theorem 4.4. □

Corollary 4.2. *Let the sensor distribution be SP3 with intensity λ on a general complex surface, the expected coverage ratio $E(f_c)$ of a FoI $\mathcal{A}_f$ with area F_f and perimeter L_f is:*

$$1-\left(1-\frac{2\pi^2r^2}{2\pi\left(\pi r^2+F_f\right)+2\pi rL_f}\right)^{\lambda\left(F_f+L_fr+\pi r^2\right)} \tag{14}$$

Proof: Please refer to the supplemental document for the detailed proof of Corollary 4.2. □

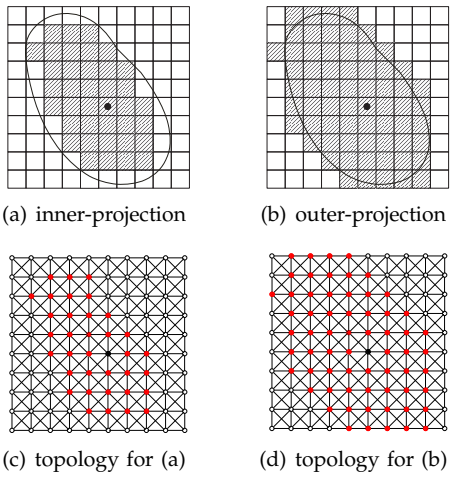

(a) inner-projection (b) outer-projection

(c) topology for (a) (d) topology for (b)

Fig. 5. An example to show the difference between inner-projection and outer-projection through top view (a)(b) and topology graphs (c)(d).

Theorem 4.5. *(for planar surface Poisson Point Process model (PP3)) Let the sensor distribution be PP3 on a general complex surface. The probability that a randomly chosen point P in $\mathcal{A}_f$ is covered by the sensor is given by:*

$$\sum_i \frac{F_i}{F_f} \frac{2\pi^2 r^2}{2\pi\left(\pi r^2 + F_i\right) + 2\pi r L_i} \frac{\left(F_i + L_i r + \pi r^2\right)\cos\theta_i}{F_f^{'} + L_f r + \pi r^2} \tag{15}$$

where θ_i is the included angle between $\mathcal{A}_i$ slant and xOy plane of the reference system and $F_f^{'}$ is the area of Z-projection of $\mathcal{A}_f$.

Proof: Please refer to the supplemental document for the detailed proof of Theorem 4.5. □

Corollary 4.3. *Let the sensor distribution be PP3 with intensity λ on a general complex surface; the expected coverage ratio $E(f_c)$ of a FoI $\mathcal{A}_f$ with area F_f and perimeter L_f is:*

$$E(f_c) = 1 - (1 - \sum_i \frac{F_i}{F_f} \frac{2\pi^2 r^2}{2\pi\left(\pi r^2 + F_i\right) + 2\pi r L_i} \frac{\left(F_i + L_i r + \pi r^2\right)\cos\theta_i}{F_f^{'} + L_f r + \pi r^2})^{\lambda\left(F_f^{'} + L_f r + \pi r^2\right)} \tag{16}$$

Proof: Please refer to the supplemental document for the detailed proof of Corollary 4.3. □

We can easily verify that the results of PP3 and SP3 are the same, and match precisely the previous result when the surface is an ideal plane, i.e. $\theta_i = 0$, $F_f^{'} = F_f = \sum_i F_i$.

Our analysis provides the methods to compute the expected coverage ratio when a given number of sensors are randomly scattered on the 3D surface. These methods could also give underlying insights for determining the appropriate number of sensors that achieves a required coverage ratio before deployment.

5 Deterministic Deployment Problem

The original optimum surface coverage problem is a difficult continuous problem. So we convert it to a discrete problem and then relate the results back to the original continuous problem. We prove the hardness of the problem and propose three algorithms offering approximate solutions.

Definition 5.1. *A* Partition *is a set defined on a surface S: $\eta = \{S_1, S_2, \ldots, S_k\}$ which satisfies: $S_i \subseteq S (i = 1 \ldots k)$, $S_i \bigcap_{i \neq j} S_j = \emptyset$, and $\bigcup_{i=1}^{k} S_i = S$. Let $\mathcal{P}$ be the set of all the partitions. Use $Gran(\eta) = \max_{i=1\ldots k}\{\parallel S_i \parallel\}$ to denote granularity of partition η. The relation $\preceq$ is a partial semi-order relation in $\mathcal{P} \times \mathcal{P}$: $\eta_i \preceq \eta_j$ if and only if η_j is a finer partition than η_i. The function $h : \eta \rightarrow 2^{\eta}$ is a function defined on partition η. Its value is a partition set that is covered by a sensor, where the independent variable is the position of the sensor. The function $h^* : 2^{\eta} \rightarrow 2^{\eta}$ is a set function defined as: $L \subseteq \eta$, $h^*(L) = \bigcup_{t \in L} h(t)$.*

Definition 5.2. *The* topology graph of partition η *is a graph $G(V, E)$, where a vertex v_i corresponds to S_i in partition η. An edge is added between vertices v_i and v_j if S_i and S_j are neighbors to each other by sharing their border or a common point. Fig.5(c) and Fig.5(d) show the corresponding topology graphs of Fig.5(a) and Fig.5(b). The distance between two pieces in a partition is defined as the length of the shortest path between the corresponding vertices. For a sensor positioned at any piece S_i, its sensing radius R is defined as the longest distance from v_i to any other vertex within its sensing area; whereas, its sensing diameter D is defined as the longest distance between any two vertices within its sensing area.*

Definition 5.3. A feasible solution to the partition coverage problem *is defined as a set L satisfying $L \subseteq \eta$ and $h^*(L) \supseteq \eta$. The* Optimum Partition Coverage Problem (OPCP) *is defined as: minimize $|L|$, L is a feasible solution.*

To solve the OSCP, we have converted the problem from its original continuous form to a discrete one. If function g in the continuous version and function h in the discrete one are correlated, we can establish a relationship between their corresponding solutions as specified in the following lemmas.

Lemma 5.1. *For every $S_i \in$ partition η, if there exists a point k in S_i to satisfy $g(k) \supseteq h(S_i)$, any feasible solutions to the discrete version of the problem will be a feasible solution to the continuous version; For any point k in S_i, if $h(S_i) \supseteq g(k)$, any feasible solutions to the continuous version of the problem will be a feasible solution to the discrete version.*

In fact, due to the impact of the surface, the coverage area of a sensor is no longer a unit disk. The function g is determined by the characteristic of the surface. For the discrete problem, there are two mechanisms to deal with the boundary: inner-projection

and outer-projection. The values of an inner-projection function are all the pieces located within the coverage area, i.e., $g(k) \supseteq h(S_i)$. On the other hand, the values of an outer-projection function include that of inner-projection plus all the pieces located at the boundary, i.e. $h(S_i) \supseteq g(k)$. Figs 5(a) and 5(b) show the instances of the inner-projection and outer-projection for the same function g. In order to satisfy the first part of Lemma 5.1, we focus on the inner-projection function from now on to ensure that our results for the discrete problem are applicable to the continuous problem.

Lemma 5.2. *Let S_{opt} be the solution to the OSCP, η_{opt} be the solution to the OPCP under partition η, and function h be an inner-projection of function g in the OSCP. Let $\eta^1, \eta^2, \ldots, \eta^i, \ldots$ be a sequence of partitions with $\eta^i \preceq \eta^{i+1}$ and $\lim_{i\to\infty} Gran(\eta^i) = 0$. We have η^i_{opt} is monotonically decreasing as i increases and $\lim_{i\to\infty} \eta^i_{opt} = S_{opt}$.*

The above two lemmas guarantee that when the partition is fine enough, the result of the OPCP can approximate the result of the OSCP precisely. To show the hardness of the OPCP, we prove that a special case of the OPCP, called *Optimum Rectangular Grid Coverage (ORGC)* problem, is NP-complete. The ORGC problem limits the shape of the sensing area and the shape of the partition in the original partition coverage problem. Since the ORGC problem is a special case of OPCP, the latter is also NP-complete.

5.1 The hardness of the ORGC problem

Definition 5.4. The Optimum Rectangular Grid Coverage (ORGC) *problem is defined as: we consider an $N \times N$ grid $\mathcal{G}$, where each pane $E_{(i,j)} \in \mathcal{G}$ is associated with four numbers to specify its coverage rectangle $\mathcal{O}_{(i,j)}$. The ORGC problem is to find a subset $\mathcal{G}'$ that minmizes $|\mathcal{G}'|$ while satisfying: $\{\bigcup_{E_{(i,j)}\in\mathcal{G}'} \mathcal{O}_{(i,j)}\} \supseteq \mathcal{G}$.*

Theorem 5.1. *ORGC problem is NP-complete.*

Proof: Planar 3SAT (P3SAT) is 3SAT restricted to formulae B such that $G(B)$ is planar. P3SAT is NP-complete[19]. We divide the procedure of reducing from P3SAT into two steps. **Step I**, we show that there is a polynomial time computable function f which converts an instance in P3SAT to an instance in ORGC. **Step II**, we prove that:

$$w \in P3SAT \Longleftrightarrow f(w) \in ORGC \tag{17}$$

where w is an instance in P3SAT.

Please refer to the supplemental document for the detailed proof of Theorem 5.1. □

5.2 Approximation algorithms for solving the Optimum Partition Coverage Problem (OPCP)

Since the OPCP is NP-complete, we propose three algorithms to solve it approximately. Algorithm 1 is a greedy algorithm. It selects a position that can increase the covered region the most.

Algorithm 1: Greedy Algorithm for OPCP

Input : Partition $\mathcal{P}$, function h of every pieces S_i
Output: A subset $\mathcal{P}'$ of $\mathcal{P}$

$\mathcal{P}' \leftarrow \emptyset$; $\mathcal{C} \leftarrow \emptyset$;
while $\mathcal{C} \not\supseteq \mathcal{P}$ **do**
  $m \leftarrow 0, x \leftarrow 0$;
  for *every* S_i *in* $\mathcal{P} - \mathcal{P}'$ **do**
    if $|h(\mathcal{S}_i) - \mathcal{C}| > m$ **then**
      $m \leftarrow |h(\mathcal{S}_i) - \mathcal{C}|; x \leftarrow i$;
    end
  end
  $\mathcal{P}' \leftarrow \mathcal{P}' \cup \{S_x\}$; $\mathcal{C} \leftarrow \mathcal{C} \cup h(\mathcal{S}_x)$;
end

Algorithm 2: Approximation Algorithm for OPCP

Input : Partition $\mathcal{P}$, the function h of every pieces S_i
Output: A subset $\mathcal{P}'$ of $\mathcal{P}$

Divide $\mathcal{P}$ into vertical strips to generate l shifting partitions $\eta^1, \eta^2, \ldots, \eta^l$;
for *each shifting partition* η^i **do**
  for *each strip group* $\eta^i_j \in \eta^i$ **do**
    Divide η^i_j into horizontal strips to generate l shifting partitions $S\eta^1, S\eta^2, \ldots, S\eta^l$;
    for *each shifting partition* $S\eta^u$ **do**
      for *each strip group* $S\eta^u_v \in S\eta^u$ **do**
        Algorithm 2(a): Using brute-force algorithm to solve the subproblem $S\eta^u_v$ and let the result be R^u_v;
        Algorithm 2(b): Using greedy algorithm to solve the subproblem $S\eta^u_v$ and let the result be R^u_v;
      end
      $R^u \leftarrow \bigcup_{v=1}^{\lceil \frac{m}{l\times D} \rceil} R^u_v$;
    end
    $R^i_j \leftarrow \min_{|R^u|} R^u$;
  end
  $R^i \leftarrow \bigcup_{j=1}^{\lceil \frac{n}{l\times D} \rceil} R^i_j$;
end
$\mathcal{P}' \leftarrow \min_{|R^i|} R^i$;

Theorem 5.2. *Algorithm 1 is an $O(|\mathcal{P}|^2)$ time $\log(|\mathcal{P}|)$-approximation algorithm.*

Proof: Please refer to the supplemental document for the detailed proof of Theorem 5.2. □

Actually, if we assume the diameter of the sensing area is D as defined in definition 5.2, then we can make use of the "shifting strategy" proposed in paper[9] to develop an polynomial-time approximation scheme(PTAS) algorithm to solve it. The approximation ratio can be $(1+\frac{1}{\epsilon})^2$. Since it is based on divide-and-conquer idea, it can be easily implemented in a distributed manner.

The main idea of Algorithm 2 is to divide the FoI into vertical strips of width D. These strips are then considered in groups of l consecutive strips resulting in strips of width $l \times D$ each. For any fixed division into strips of width D, there are l different ways of partitioning FoI into strips of width $l \times D$. These partitions can be ordered such that each can be derived from the previous one by shifting it to the right over distance D. We use the same method to solve the subproblem and output the union of all positions. For l different shifting partitions, we select the optimum result as the final result.

The main framework and some symbols can refer to [9]. Especially, Algorithm 2 includes two alternative parts: Algorithm 2(a) and Algorithm 2(b). The most pseudo-codes of these two algorithms are the same. The difference is that Algorithm 2(a) only carries out Line 7 but not Line 8 and Algorithm 2(b) only operates Line 8 but not Line 7.

Theorem 5.3. *Algorithm 2(a) is an* $O(\frac{|\mathcal{P}|}{D^2} \times 2^{l^2D^2})$ *time* $(1+\frac{1}{l})^2$*-approximation algorithm.*

Proof: Please refer to the supplemental document for the detailed proof of Theorem 5.3. □

Although the performance ratio looks fine, it may be not practical in real environments because even $l = 1$ is a big cost since D is often larger than five. We sacrifice some accuracy to reduce the cost of calculation. This brings us to algorithm 2(b). It mixes the core idea in algorithm 1 and algorithm 2(a) and simply uses the greedy algorithm (Line 8 in Algorithm 2) instead of the brute-force algorithm (Line 7 in Algorithm 2). It can still be implemented in a distributed manner. We call it algorithm 2(b).

Theorem 5.4. *Algorithm 2(b) is an* $O(|\mathcal{P}|l^4D^2)$ *time* $\log(l^2D^2) \times (1+\frac{1}{l})^2$*-approximation algorithm.*

Proof: Please refer to the supplemental document for the detailed proof of Theorem 5.4. □

6 Performance Evaluation

The main purpose of the evaluation is to: (i) point out the limitation of the traditional methods, (ii) verify our derived results, and (iii) make comparisons of the three proposed algorithms in a comprehensive manner.

We utilize Terragen [2], a professional terrain generating tool to simulate surface, and the widely-used "Ridged Perlin Noise" to generate a natural, ridged landscape. Glaciation is a widely-used parameter to measure the steepness of a terrain [2]. A low Glaciation generates a smoothly flat terrain as shown in Fig.6(a). On the contrary, a high Glaciation generates a sharply fluctuant terrain as shown in Fig.6(b). We use triangularization to partition a surface for our evaluation. Fig.6(c) depicts surface triangularization.

There are several methods for covering the FoI if the FoI is an ideal 2D plane. The typical one is the triangle pattern [14]. Thus, we take this method as the representative pattern for performance evaluation. Six different terrains are generated, whose Glaciation is set 0, 20, 40, 60, 80, and 100 respectively. All sensors can be only deployed on the surface. In this simulation, the size of the FoI is set to be $1920 \times 1920m^2$. The height range is from $300m$ to $2000m$ and the sensing radius is $30m$. Finally, we calculate the coverage ratio. Fig.7 presents the performance of the typical triangle pattern. The number of sensors is set to satisfy the minimum value for achieving full coverage (the coverage ratio is 1) when $Glaciation = 0$. When the parameter Glaciation increases, the coverage ratio decreases quickly. It drops to about 60% when $Glaciation = 100$. Hence, the conventional triangle pattern does not work well on a complex surface. It is necessary to find new methods to cover the complex surface.

Fig.8 shows the coverage ratio under stochastic distribution. The solid lines present the theoretical results calculated by the proposed methods in Section 4. And the dash lines present the experimental results obtained by our simulation, which we stochastically deploy sensors on the surface and do the statistics of the coverage ratio. We find that the theoretical results match the experimental results precisely, no matter the Glaciation is low or high. Fig.8 demonstrates the validity of our method to calculate the coverage ratio under stochastic distribution on complex surface.

Fig.9 compares the results of the three proposed algorithms under deterministic deployment. We utilize a square partition in our experiment because the terrain file is a dot matrix and can be easily converted to a square partition. The FoI is a $N \times N$ grid, where N is the distance measured by partitions. The X-axis is the side length of the FoI and the Y-axis means how many sensors are needed to have a complete coverage (coverage ratio is 1) of the FoI. The performance of the simple greedy algorithm provides the best result, which demands the minimum number of sensors for complete coverage. Algorithm 2(a) has the best theoretical performance bound when l (refer to Section 5.2) is large enough. Unfortunately, the time complexity is exponential as l increases. Thus, it can only be executed effectively when $l = 1$ and $D \leq 5$ (refer to Definition 5.2). However, the small D implicates that the size of the partition is large. We must guarantee that the partition is detailed enough to get a precise solution to the original OSCP as stated in lemma 5.2. In Fig.9, D is set to be 3 so that we can compare Algorithm 2(a) with other algorithms. We find that the results of Algorithm 2(a) and 2(b) ($l = 1$) is close. Furthermore, the number of sensors decreases when l increases for Algorithm 2(b).

The experiment of Fig.10 is similar to Fig.9, but the sensing diameter is changed to $D = 7$. Fig.10 also compares the three proposed algorithms. The performance of algorithm 1 is still the best. Note that

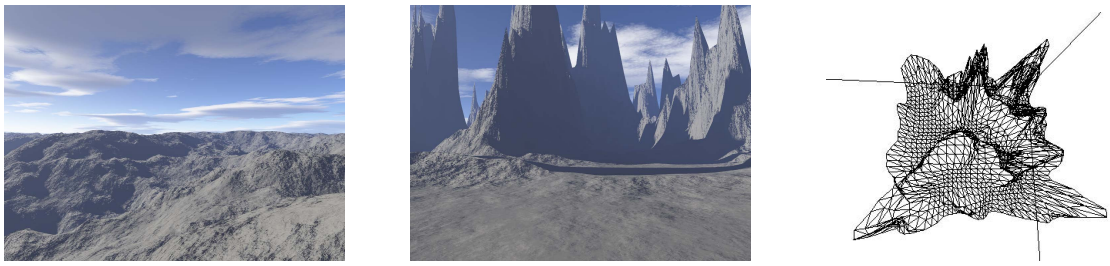

(a) (b) (c)

Fig. 6. (a) Terrain1 with Glaciation=20 generated by Terragen[2]. (b) Terrain2 with Glaciation=100. (c). Terrain2 after triangularization (Top view).

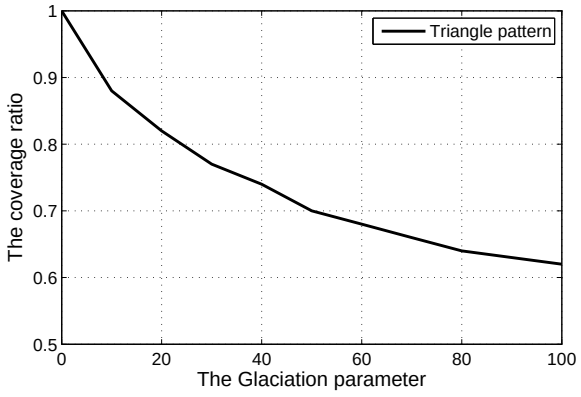

Fig. 7. The sensors fully cover a plane FoI (Glaciation=0). But the coverage ratio drops when Glaciation increases. This simulation demonstrates that it is necessary to study the surface coverage problem.

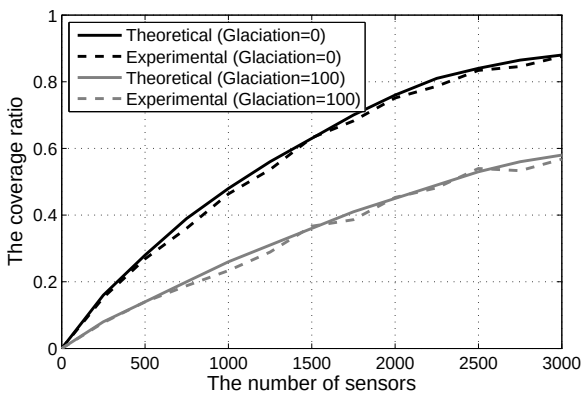

Fig. 8. The expected coverage ratio in stochastic distribution case. We compare the theoretical value calculated by our proposed method and the experimental value obtained in the simulation.

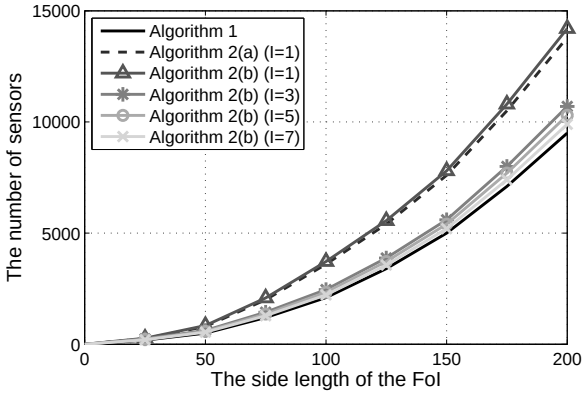

Fig. 9. In deteminstic deployment case, the minimum number of sensors satisfies the full coverage of a FoI with given side length. The results are obtained by our proposed algorithms when sensing diameter $D = 3$.

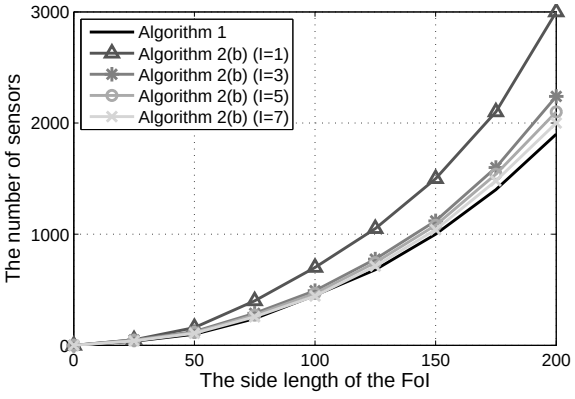

Fig. 10. In deteminstic deployment case, the minimum number of sensors satisfies the full coverage of a FoI with given side length. The results are obtained by our proposed algorithms when sensing diameter $D = 7$.

algorithm 2(a) and algorithm 2(b) can be implemented in a distributed manner, and we propose algorithm 2(b) because the calculation cost of algorithm 2(a) is too large.

The results tell us that algorithm 1 is the best choice. Although its theoretical performance bound is not very acceptable, its average approximation ratio is precise enough.

7 Discussions

In this section, we discuss some practical issues.

(i) *Surface is not a single-valued function (i.e. not convex).* Note that our solution only depends on a partition of the surface. If we have proper expressions

of the surface when it is not a single-valued function, we can partition it and our solution can still be applied.

(ii) *The errors between a smooth surface and a surface with triangles.* Due to discrepancy between a smooth surface and a triangulated surface, unavoidable errors that occur when converting a smooth surface into a triangulated one are minimized when the triangles are small. Since geographic information systems (GIS) provide data in a dot matrix, accuracy is lost in this data storage system, and not in the calculation process.

(iii) *Relationship between surface parameter and coverage ratio.* After a survey of the current surface parameters in the GIS, we have not found any relative parameters. The impact on coverage ratio is the ratio of the area to the projective area. In general, a terrain with more mountains and densely populated with mountains will have a relatively poor coverage ratio.

8 Conclusions and Future Work

We have proposed a new model for the coverage problem called surface coverage to better capture real world application challenges. Two problems pertaining to surface coverage were in focus: the expected coverage ratio with stochastic deployment and the optimal deployment strategy with planned deployment. Comprehensive simulation experiments show that though the performance bound of the greedy algorithm is not the best, it often outperforms the other two algorithms. To our best knowledge, this is the first attempt to describe and resolve the surface coverage problem in WSNs.

Future research can be carried out following many directions. For instance, our research considers only static sensors. Mobile sensors for surface coverage is worthy to further study. Moreover, the connectivity problem is still an open problem in surface coverage domain.

Acknowledgements

This research was supported by NSF of China under grant No. 60773091, 973 Program of China under grant No. 2006CB303000, 863 Program of China under grant No. 2006AA01Z247, Innovation program of SJTU under grant No. Z-030-022, Hong Kong RGC Grants HKUST617908 and HKBU 1/05C, the Key Project of China NSFC Grant 60533110. Our shepherd, Jin-Yi Cai, Xiang-Yang Li, Dong Xuan, Ten H. Lai, Lionel M. Ni gave us highly valuable comments.

References

[1] http://fiji.eecs.harvard.edu/Volcano/.
[2] http://www.planetside.co.uk/terragen/.
[3] X. Bai, D. Xuan, Z. Yun, T. H. Lai, and W. Jia. Complete optimal deployment patterns for full-coverage and k-connectivity (k≤6) wireless sensor networks. In *ACM MobiHoc*, pages 401–410, New York, NY, USA, 2008.
[4] P. Balister, B. Bollobas, A. Sarkar, and S. Kumar. Reliable density estimates for coverage and connectivity in thin strips of finite length. In *ACM MobiCom*, pages 75–86, New York, NY, USA, 2007.
[5] Y. Bejerano. Simple and efficient k-coverage verification without location information. *IEEE INFOCOM*, pages 291–295, April 2008.
[6] M. Cardei, M. Thai, Y. Li, and W. Wu. Energy-efficient target coverage in wireless sensor networks. *IEEE INFOCOM*, 3:1976–1984 vol. 3, March 2005.
[7] A. Chen, S. Kumar, and T. H. Lai. Designing localized algorithms for barrier coverage. In *ACM MobiCom*, pages 63–74, New York, NY, USA, 2007.
[8] P. Corke, S. Hrabar, R. Peterson, D. Rus, S. Saripalli, and G. Sukhatme. Autonomous deployment and repair of a sensor network using an unmanned aerial vehicle. *IEEE ICRA*, 4:3602–3608 Vol.4, 26-May 1, 2004.
[9] D. S. Hochbaum and W. Maass. Approximation schemes for covering and packing problems in image processing and vlsi. *J. ACM*, 32(1):130–136, 1985.
[10] C.-F. Huang, Y.-C. Tseng, and L.-C. Lo. The coverage problem in three-dimensional wireless sensor networks. *IEEE GLOBECOM*, 5:3182–3186 Vol.5, Nov.-3 Dec. 2004.
[11] R. Iyengar, K. Kar, and S. Banerjee. Low-coordination topologies for redundancy in sensor networks. In *ACM MobiHoc*, pages 332–342, New York, NY, USA, 2005.
[12] M. Jin, G. Rong, H. Wu, L. Shuai, and X. Guo. Optimal surface deployment problem in wireless sensor networks. In *INFOCOM, 2012 Proceedings IEEE*, pages 2345–2353. IEEE, 2012.
[13] K. Kar and S. Banerjee. Node placement for connected coverage in sensor networks. *WiOpt*, pages 1–10, April 2003.
[14] R. Kershner. The number of circles covering a set. *American Journal of Mathematics*, 1939.
[15] L. Kong, D. Jiang, and M. Wu. Optimizing the spatio-temporal distribution of cyber-physical systems for environment abstraction. In *IEEE Distributed Computing Systems (ICDCS)*, pages 179–188, 2010.
[16] S. Kumar, T. H. Lai, and A. Arora. Barrier coverage with wireless sensors. In *ACM MobiCom*, pages 284–298, New York, NY, USA, 2005.
[17] L. Lazos and R. Poovendran. Stochastic coverage in heterogeneous sensor networks. *ACM Trans. Sen. Netw.*, 2(3):325–358, 2006.
[18] X.-Y. Li, P.-J. Wan, and O. Frieder. Coverage in wireless ad hoc sensor networks. *IEEE Transactions on Computers*, 52(6):753–763, June 2003.
[19] D. Lichtenstein. Planar formulae and their uses. *SIAM Journal on Computing*, 11(2):329–343, 1982.
[20] B. Liu, P. Brass, O. Dousse, P. Nain, and D. Towsley. Mobility improves coverage of sensor networks. In *ACM MobiHoc*, pages 300–308, New York, NY, USA, 2005.
[21] L. Liu and H. Ma. On coverage of wireless sensor networks for rolling terrains. *Parallel and Distributed Systems, IEEE Transactions on*, 23(1):118–125, 2012.
[22] S. Meguerdichian, F. Koushanfar, M. Potkonjak, and M. Srivastava. Coverage problems in wireless ad-hoc sensor networks. *IEEE INFOCOM*, 3:1380–1387 vol.3, 2001.
[23] L. A. SANTALO. *Integral geometry and geometric probability*. Addison-Wesley, Massachusetts (etc.), 1976.
[24] W. W. V. Srinivasan and K.-C. Chua. Trade-offs between mobility and density for coverage in wireless sensor networks. In *ACM MobiCom*, pages 39–50, New York, NY, USA, 2007.
[25] X. Wang, G. Xing, Y. Zhang, C. Lu, R. Pless, and C. Gill. Integrated coverage and connectivity configuration in wireless sensor networks. In *ACM SenSys*, pages 28–39, New York, NY, USA, 2003.
[26] M. Watfa and S. Commuri. A coverage algorithm in 3d wireless sensor networks. *IEEE PerCom*, pages 6 pp.–, Jan. 2006.
[27] H. Zhou, H. Wu, S. Xia, M. Jin, and N. Ding. A distributed triangulation algorithm for wireless sensor networks on 2d and 3d surface. In *INFOCOM, 2011 Proceedings IEEE*, pages 1053–1061. IEEE, 2011.

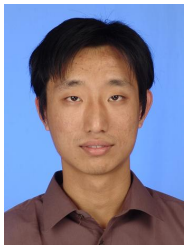

Linghe Kong received his B. E. degree in Automation Department from Xidian University, China, in 2005. He received his Dipl. Ing. degree in Telecommunication from TELECOM SudParis (ex. INT), France, in 2007. He is currently working toward the PhD degree in Department of Computer Science and Engineer in Shanghai Jiao Tong University with Prof. Min-You WU. His research interests are in the area of wireless sensor networks and cyber-physical systems.

Mingchen Zhao is a second-year Ph.D. student in the Computer and Information Science Department of University of Pennsylvania. Supervised by Prof. Andreas Haeberlen, he mainly works on security problems in distributed systems. Previously, Mingchen obtained his Bachelor of Engineering degree and Master of Engineering degree from the Computer Science and Engineering Department of Shanghai Jiao Tong University, under the supervision of Prof. Min-You Wu.

Xiao-Yang Liu received his B. E. degree in computer science in Huazhong University of Science and Technology, China, in 2009. He is currently working toward the PhD degree in Department of Computer Science and Engineer in Shanghai Jiao Tong University with Prof. Min-You WU. His research interests are in the area of wireless sensor networks.

Jialiang Lu received his Master and Ph.D degree in INSA Lyon, France, in 2008. He is currently a assistant researcher in Department of Computer Science and Engineer in Shanghai Jiao Tong University. His research interests are in the area of wireless sensor networks.

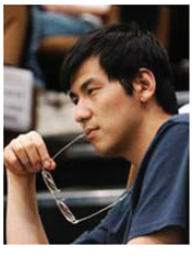

Yunhuai Liu earned his B.S. degree from computer science and technology department of Tsinghua University in July, 2000. Then he got his first job in Hewlett Packard (China) in Beijing as a system engineer. After nearly three years of working with HP, he began to pursuit his Ph.D at computer science department in Hong Kong University of Science and Technology. In July 2008, he passed the final defense of PHD. After that, he worked as an research assistant professor in Hong Kong University of Science and Technology. In 2010 Aug he joined the institute of advanced computing and digital engineering, Shenzhen Institutes of Advanced echnology (SIAT), Chinese Academy of Sciences (CAS) to start a new career. He is now an associate researcher.

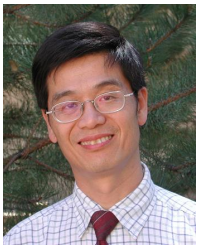

Min-You Wu (S'84-M'85-SM'96) received the M.S. degree from the Graduate School of Academia Sinica, Beijing, China, in 1981 and the Ph.D. degree from Santa Clara University, Santa Clara, CA in 1984. He is a professor in the Department of Computer Science and Engineering at Shanghai Jiao Tong University and a research professor with the University of New Mexico. He serves as the Chief Scientist at Grid Center of Shanghai Jiao Tong University. His research interests include grid computing, wireless networks, sensor networks, multimedia networking, parallel and distributed systems, and compilers for parallel computers.

Wei Shu (M'90-SM'99) received the Ph.D. degree from the University of Illinois at UrbanaCChampaign. She was with the Yale University, New Haven, CT, the State University of New York at Buffalo, and the University of Central Florida, Orlando. She is currently an Associate Professor with the Department of Electrical and Computer Engineering, University of New Mexico, Albuquerque. Her current research interests include resource management, multimedia networking, distributed systems, wireless networks, and sensor networks.

Supplemental Document: Surface Coverage in Sensor Networks

Linghe Kong, Mingchen Zhao, Xiao-Yang Liu,
Jialiang Lu, *Member, IEEE,* Yunhuai Liu, *Member, IEEE,*
Min-You Wu, *Senior Member, IEEE,* Wei Shu, *Senior Member, IEEE,*

Abstract—This manuscript includes the supplementary sections for the paper titled "Surface Coverage in Sensor Networks". It provides the section of proofs and the section of problem extension.

1 PROOF

Theorem 4.1. *Let $\mathcal{A}_f$ be a FoI of area F_f and perimeter L_f on a plane, and let every sensor $\mathcal{A}_s$ have the same sensing radius r. N sensors are stochastically placed on the plane in such a way that it intersects with $\mathcal{A}_f$ according to PP3 model or SP3 model. The expected coverage ratio $E(f_c)$ of the FoI $\mathcal{A}_f$ is given by:*

$$1-\left(1-\frac{2\pi^2r^2}{2\pi\left(\pi r^2+F_f\right)+2\pi rL_f}\right)^N$$

Proof: According to Lemma 3.3, when $\mathcal{A}_1$ and $\mathcal{A}_0$ are intersected. The probability that a randomly selected point $P\in\mathcal{A}_0$ is covered by $\mathcal{A}_1$ is

$$p(P\in\mathcal{A}_1)=\frac{2\pi F_1}{2\pi(F_0+F_1)+L_0L_1}.$$

Substitute $\mathcal{A}_0$ by $\mathcal{A}_f$ and $\mathcal{A}_1$ by $\mathcal{A}_s$ in above equation. The coverage area of a sensor F_s is πr^2 and its perimeter L_s is $2\pi r$. Thus, the probability that a randomly selected point $P\in\mathcal{A}_f$ is covered by $\mathcal{A}_s$ is:

$$\frac{2\pi^2r^2}{2\pi(F_f+\pi r^2)+2\pi rL_f}.$$

Then, the probability that a randomly selected point $P\in\mathcal{A}_f$ is not covered by $\mathcal{A}_s$ is

$$p(P\notin\mathcal{A}_s)=1-\frac{2\pi^2r^2}{2\pi(F_f+\pi r^2)+2\pi rL_f}.$$

Since N sensors are randomly scattered on $\mathcal{A}_f$, the expected coverage ratio is:

$$1-\left(1-\frac{2\pi^2r^2}{2\pi\left(\pi r^2+F_f\right)+2\pi rL_f}\right)^N.$$

□

Corollary 4.1. *Let $\mathcal{A}_f$ be a FoI of area F_f and perimeter L_f on a plane. Let the distribution of the sensors with sensing radius r be PP3 model or SP3 model with intensity λ. The expected coverage ratio $E(f_c)$ of the FoI $\mathcal{A}_f$ is:*

$$1-\left(1-\frac{2\pi^2r^2}{2\pi\left(\pi r^2+F_f\right)+2\pi rL_f}\right)^{\lambda\left(F_f+L_fr+\pi r^2\right)}$$

Proof: The main process to derive Corollary 4.1 is similar to Theorem 4.1. The only difference is to replace *'random deploying N sensors'* by *'all sensors are randomly distributed with intensity λ'*. Hence, the exponent is $\lambda\left(F_f+L_fr+\pi r^2\right)$ instead of N when computing the expected coverage ratio. Then, this Corollary is immediately obtained.

□

Theorem 4.2. *Let $\mathcal{A}_f$ be a FoI of area F_f and perimeter L_f on a slant. Let the distribution of the sensors with sensing radius r be SP3 model with intensity λ. The expected coverage ratio $E(f_c)$ of the FoI $\mathcal{A}_f$ is:*

$$1-\left(1-\frac{2\pi^2r^2}{2\pi\left(\pi r^2+F_f\right)+2\pi rL_f}\right)^{\lambda\left(F_f+L_fr+\pi r^2\right)}$$

Proof: SP3 in a slant is similar to PP3 in a plane after some rotation of the reference system. So, the result is same with Corollary 4.1.

□

Theorem 4.3. *Let $\mathcal{A}_f$ be a FoI of area F_f and perimeter L_f on a slant whose equation can be expressed as $z=ax+by+c$. Let the distribution of the sensors with sensing radius r be PP3 model with intensity λ. The expected coverage ratio $E(f_c)$ of the FoI $\mathcal{A}_f$ is:*

$$1-\left(1-\frac{2\pi^2r^2}{2\pi\left(\pi r^2+F_f\right)+2\pi rL_f}\right)^{\lambda\cos\theta\left(F_f+L_fr+\pi r^2\right)}$$

where

$$\theta=\arccos\left(\frac{1}{\sqrt{a^2+b^2+1}}\right)\qquad 0\le\theta<\frac{\pi}{2}$$

Proof: PP3 with intensity λ can be considered as SP3 with intensity $\lambda\cos\theta$. By combining Corollary 4.1 and Lemma 4.1, the result is obtained.

□

Theorem 4.4. *(for space surface Poisson Point Process model (SP3)) Let the sensor distribution be SP3 on a general complex surface. The probability that a randomly chosen point P in $\mathcal{A}_f$ is covered by the sensor is given by:*

$$p(P\in\mathcal{A}_s)=\frac{2\pi^2r^2}{2\pi\left(\pi r^2+F_f\right)+2\pi rL_f}$$

Proof:

$$\begin{aligned} & p(P \in \mathcal{A}_s) \\ = & \sum_i p(P \in \mathcal{A}_s \mid P \in \mathcal{A}_i) p(P \in \mathcal{A}_i) \\ = & \sum_i \frac{F_i}{F_f} \frac{2\pi F_s}{2\pi (F_s + F_i) + L_s L_i} \frac{2\pi (F_s + F_i) + L_s L_i}{2\pi (F_s + F_f) + L_s L_f} \\ = & \frac{2\pi^2 r^2}{2\pi (\pi r^2 + F_f) + 2\pi r L_f} \end{aligned}$$

□

Corollary 4.2. *Let the sensor distribution be SP3 with intensity λ on a general complex surface, the expected coverage ratio $E(f_c)$ of a FoI $\mathcal{A}_f$ with area F_f and perimeter L_f is:*

$$1 - \left(1 - \frac{2\pi^2 r^2}{2\pi (\pi r^2 + F_f) + 2\pi r L_f}\right)^{\lambda\left(F_f + L_f r + \pi r^2\right)}$$

Proof: Combining Theorem 4.2 and Theorem 4.4, the result can be obtained.

□

Theorem 4.5. *(for planar surface Poisson Point Process model (PP3)) Let the sensor distribution be PP3 on a general complex surface. The probability that a randomly chosen point P in $\mathcal{A}_f$ is covered by the sensor is given by:*

$$\sum_i \frac{F_i}{F_f} \frac{2\pi^2 r^2}{2\pi (\pi r^2 + F_i) + 2\pi r L_i} \frac{\left(F_i + L_i r + \pi r^2\right) \cos\theta_i}{F_f^{'} + L_f r + \pi r^2}$$

where θ_i is the included angle between $\mathcal{A}_i$ plane and xOy plane of the reference system and $F_f^{'}$ is the area of Z-projection of $\mathcal{A}_f$.

Proof:

$$\begin{aligned} p(P \in \mathcal{A}_s) &= \sum_i p(P \in \mathcal{A}_s \mid P \in \mathcal{A}_i) p(P \in \mathcal{A}_i) \\ &= \sum_i p(P \in \mathcal{A}_i) \\ &\quad p(P \in \mathcal{A}_s \mid P \in \mathcal{A}_i, \mathcal{A}_i \cap \mathcal{A}_s \neq \emptyset) \\ &\quad p(\mathcal{A}_i \cap \mathcal{A}_s \neq \emptyset) \\ &= \sum_i \frac{F_i}{F_f} \frac{2\pi^2 r^2}{2\pi (\pi r^2 + F_i) + 2\pi r L_i} \\ &\quad \frac{\left(F_i + L_i r + \pi r^2\right) \cos\theta_i}{F_f^{'} + L_f r + \pi r^2} \end{aligned}$$

□

Corollary 4.3. *Let the sensor distribution be PP3 with intensity λ on a general complex surface; the expected coverage ratio $E(f_c)$ of a FoI $\mathcal{A}_f$ with area F_f and perimeter L_f is:*

$$\begin{aligned} E(f_c) = & 1 - (1 - \sum_i \frac{F_i}{F_f} \frac{2\pi^2 r^2}{2\pi (\pi r^2 + F_i) + 2\pi r L_i} \\ & \frac{\left(F_i + L_i r + \pi r^2\right) \cos\theta_i}{F_f^{'} + L_f r + \pi r^2})^{\lambda\left(F_f^{'} + L_f r + \pi r^2\right)} \end{aligned}$$

TABLE 1
Notations for NP-Complete Proof

Symbol	Definition
N	The length of the grid;
m	The number of clauses in an instance of P3SAT;
n	The number of variables in an instance of P3SAT;
t_i	The number of appearances of the ith variable, where i satisfies $1 \leq i \leq n$;
e	The number of edges between clauses and literals, which is calculated by $\sum_{i=1}^{n} t_i$;
p_j	The number of panes on the jth path ($1 \leq j \leq e$).

Proof: Combining Theorem 4.2 and Theorem 4.5, the result can be obtained.

□

Theorem 5.1. ORGC problem is NP-complete.

Proof: Before the proof of Theorem 4.1, a definition is given.

Definition 5.5. The k determination of the ORGC problem: *given a grid $\mathcal{G}$, determine if there exists a cover set $\mathcal{G}' \subseteq \mathcal{G}$ satisfying $|\mathcal{G}'| = k$ and $\{\bigcup_{E_{(i,j)} \in \mathcal{G}'} \mathcal{O}_{(i,j)}\} \supseteq \mathcal{G}$.*

If pane $E_{(x,y)}$ associated with (a_1, a_2, a_3, a_4) is selected, it can cover $\mathcal{O}_{(x,y)}$, a rectangular area from pane $E_{(x-a_1, y+a_2)}$ to pane $E_{(x+a_3, y-a_4)}$. For example, if we have pane $E_{(1,1)}$ associated with $(0, 1, 1, 1)$, it can cover $\mathcal{O}_{(1,1)}$, a rectangle from pane $E_{(1,2)}$ to pane $E_{(2,0)}$ as shown in Fig.2(a).

Planar 3SAT (P3SAT) is 3SAT restricted to formulae B such that $G(B)$ is planar. P3SAT is NP-complete[4]. We divide the procedure of reducing from P3SAT into two steps. **Step I**, we show that there is a polynomial time computable function f which converts an instance in P3SAT to an instance in ORGC. **Step II**, we prove that:

$$w \in P3SAT \Longleftrightarrow f(w) \in ORGC$$

where w is an instance in P3SAT.

Step I in detail: we describe the polynomial time computable function f. Fig.2(b) shows an instance of formulae $(x \vee y \vee z) \wedge (\bar{x} \vee y \vee z)$. It is made up of three basic elements: clause nodes, variable nodes, and edges. We convert them separately into gadgets according to the following rules.

• We select a sufficiently large N to guarantee that any two gadgets will not overlap and that their edges can be substituted by rectilinear paths. The planarity of P3SAT guarantees that no two paths will crossover. For convenience, we use a rectangular area and a point instead of the four numbers to indicate the area to be covered.

• For each clause, we convert it to a gadget as shown in Fig.1(a). A, B, C are three connection points which must be connected with the path from the literal occurring in the clause.

• For variable i which occurs t_i times, we convert it to a gadget shown in Fig.1(b) and 1(c) with length of $(6t_i + 1)$.

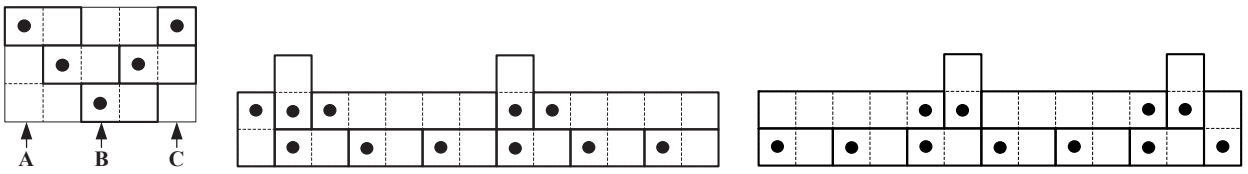

(a) clause gadget. (b) variable gadget1. (c) variable gadget2.

Fig. 1. Clause gadget and variable gadget in P3SAT problem.

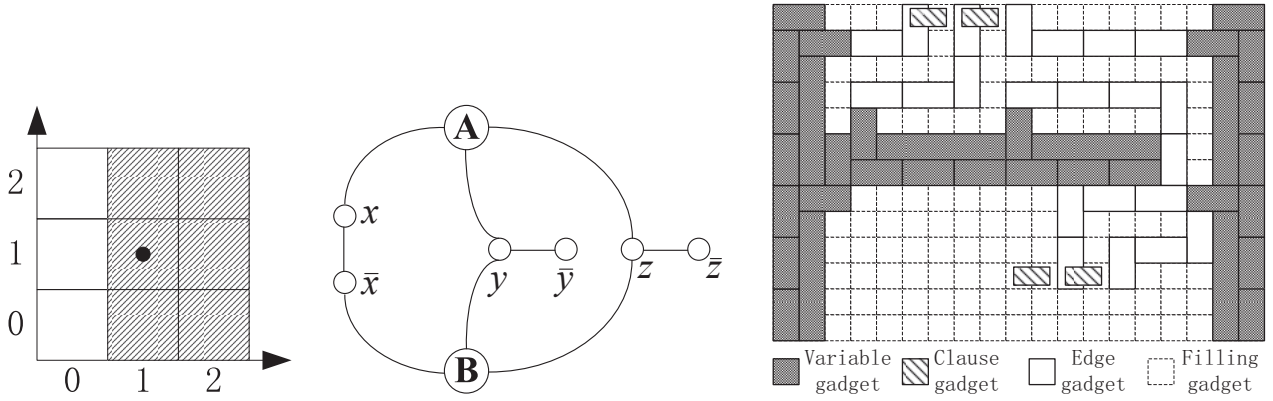

(a) (b) (c)

Fig. 2. (a) The concept of a covered region in ORGC. (b) The instance of P3SAT. (c) The instance of a converted ORGC.

• For the paths, we convert them to a series of 1×2 dominos. If the length of a path is odd, we add a 1×3 domino to guarantee that the total dominos used to propagate satisfiable assignment is $\lfloor \frac{p_j}{2} \rfloor$.

We use 1×1 dominos to fill other blank areas. The time complexity needed to convert the planar graph to a rectangular grid coverage problem is polynomial. The corresponding instance of ORGC is shown in Fig.2(c).

Step II in detail: For the clause gadget, we can easily verify the following properties:

• If any true assignment is not propagated to a clause gadget (none of three connection points is covered), it must be covered by three dominoes. Otherwise, it can be covered by two dominoes.

• Even if all three variables are true, it still needs two dominoes to cover the area.

For the variable gadget, the first case in Fig.1(b) means X_i is assigned a true value; the second case in Fig.1(c) means X_i is assigned a false value. We can easily verify the following properties: for a gadget of length $(6t_i + 1)$ (means total $2 \times (6t_i + 1)$ panes), it needs at least $(5t_i+1)$ dominoes to cover the full area. If each occurrence of a literal is consistent, we can use $(5t_i + 1)$ dominoes to fully cover the area. Otherwise, more than $(5t_i + 1)$ dominoes are required to fully cover the area.

For the paths, whatever its length, we can use $\sum_{j=1}^{e} \lfloor \frac{p_j}{2} \rfloor$ dominoes to propagate the satisfiable assignment.

Based on the above properties, for an instance of P3SAT, there must be a consistent assignment to all the variables that satisfy all the clauses. The total number of dominoes is: $R = N^2 - [\sum_{i=1}^{n}(7t_i + 1)] - 3m - \sum_{j=1}^{e} \lceil \frac{p_j}{2} \rceil$. Next, if a grid can be covered by selecting R panes, the minimum coverage of every gadget is achieved. We know that each clause is covered by two dominoes. It implies that there must be no fewer than one satisfied assignment. So the corresponding instance is satisfiable. Hence,

$$w \in P3SAT \Longleftrightarrow f(w) \in ORGC$$

is proved.

□

Theorem 5.2. *Algorithm 1 is an $O(|\mathcal{P}|^2)$ time $\log(|\mathcal{P}|)$-approximation algorithm.*

Proof: Let $\mathcal{C}_i$ denote the partition set $\mathcal{C}$ after the ith turn selection of the algorithm 1. Let $\mathcal{NC}_i$ denote the set of newly covered panes in turn i. Actually, $\mathcal{NC}_i = h(\mathcal{S}_i) - \mathcal{C}_{i-1}$, where $\mathcal{S}_i$ is the selected piece of turn i. $|\mathcal{P}|$ is the total pieces of the partition $\mathcal{P}$. $\mathcal{P}_{opt}$ is the optimal selection of panes, i.e. the optimal solution to OPCP problem. Let $\mathcal{P}'_{opt}$ be the current optimal solution after some pieces has been covered. Obviously, $|\mathcal{P}'_{opt}| \leq |\mathcal{P}_{opt}|$. Then we have:

$$\frac{1}{|\mathcal{NC}_i|} \leq \frac{|\mathcal{P}'_{opt}|}{|\mathcal{P}| - |\mathcal{C}_{i-1}|} \leq \frac{|\mathcal{P}_{opt}|}{|\mathcal{P}| - |\mathcal{C}_{i-1}|}$$

Finally, for our solution k, we have

$$k = \sum_{i=1}^{k} |\mathcal{NC}_i| \frac{1}{|\mathcal{NC}_i|}$$

$$\leq \frac{|\mathcal{P}_{opt}|}{|\mathcal{P}|} + \frac{|\mathcal{P}_{opt}|}{|\mathcal{P}|-1} + \ldots + \frac{|\mathcal{P}_{opt}|}{1}$$
$$= |\mathcal{P}_{opt}| \sum_{i=1}^{|\mathcal{P}|} \frac{1}{i}$$

Since $\sum_{i=1}^{N} \frac{1}{i}$ is the harmonic series, its value is $\ln(n+1)+r$ where r is the Euler constant. Then we have:

$$k \leq |\mathcal{P}_{opt}|(\ln(|\mathcal{P}|+1)+r) \leq |\mathcal{P}_{opt}|(\ln(|\mathcal{P}|)+1)$$

From this equation, we derive our conclusion. □

Theorem 5.3. *Algorithm 2(a) is an $O(\frac{|\mathcal{P}|}{D^2} \times 2^{l^2D^2})$ time $(1+\frac{1}{l})^2$-approximation algorithm.*

Proof: We analyze Algorithm 2(a) by dividing it into two parts: shifting strategy part and optimum searching part. In [2], the authors have proved that the shifting strategy part is an $O(\frac{|\mathcal{P}|}{D^2})$ time $(1+\frac{1}{l})^2$-approximation algorithm. In Algorithm 2(a), the optimum searching part adopts the brute-force method. This method can obtain the optimum result with no error by enumeration and its time complexity is easy to obtain $O(2^{l^2D^2})$. Combining these two parts, the time complexity and approximation of Algorithm 2(a) are obtained. □

Theorem 5.4. *Algorithm 2(b) is an $O(|\mathcal{P}|l^4D^2)$ time $\log(l^2D^2) \times (1+\frac{1}{l})^2$-approximation algorithm.*

Proof: Algorithm 2(b) is also divided into shifting strategy part and optimum searching part. The shifting strategy part is an $O(\frac{|\mathcal{P}|}{D^2})$ time $(1+\frac{1}{l})^2$-approximation algorithm, which is same with Theorem 4.3. In Algorithm 2(b), the optimum searching part adopts the greedy method. Its time complexity is $O((l^2D^2)^2)$ and approximation is $\log(l^2D^2)$. Combining the time complexity and approximation of two parts, Theorem 5.4 is proved. □

2 Problem Extension

The above study focuses on the problem scope that the FoI is finite surface without hole, the sensors are static with homogeneous sensing area, the distribution is deterministic or stochastic (PP3, SP3), the requirement is full coverage without the limitation of connectivity. In this section, we extend our methods to other cases in the problem scope.

2.1 Extend to *FoI* with Holes

Fig.3(a) shows a mountain with a lake, which is a typical case of a FoI with hole. Fig.3(b) shows its topology projection from top view. FoIs with holes are normal in the real WSN application such as lakes and obstacles.

In the stochastic distribution case, the coverage ratio is calculated based on the following Theorem.

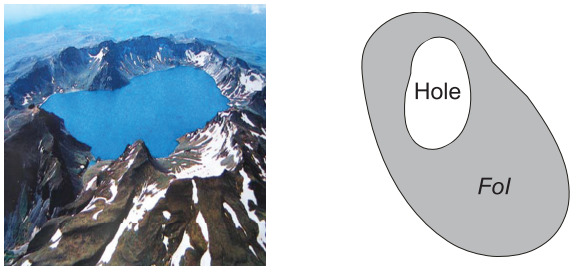

(a) (b)

Fig. 3. (a) A mountain with a lake. (b) The topology graph of FoI with a hole through top views.

Theorem S2.1. *Let $\mathcal{A}_s$ denote a sensor of area F_s and perimeter L_s. And let $\mathcal{A}_f$ denote a FoI with holes, with $\mathcal{A}_f$ being the union of a finite number of separate convex regions $\mathcal{A}_f^i, i = 1, 2, \cdots \phi$, of total area F_f and total perimeter L_f. The probability that a randomly selected point P in $\mathcal{A}_f$ is covered by $\mathcal{A}_s$ is given by*

$$p(P \in \mathcal{A}_s) = \frac{2\pi\phi F_s}{2\pi(F_f + \phi F_s) + L_f L_s}. \quad (1)$$

Proof: Book [5] gives the Theorem: Let $\mathcal{A}_1$ being a convex set with the area F_1 and perimeter L_1. Let $\mathcal{A}_0$ being the union of a finite number of separate convex regions $\mathcal{A}_0^i, i = 1, 2, \cdots \phi$, of total area F_0 and total perimeter L_0. The probability that a randomly selected point P in $\mathcal{A}_0$ is covered by $\mathcal{A}_1$ is:

$$p(P \in \mathcal{A}_1) = \frac{2\pi\phi F_1}{2\pi(F_0 + \phi F_1) + L_0 L_1}. \quad (2)$$

Substituting $\mathcal{A}_0$ by $\mathcal{A}_f$ and $\mathcal{A}_1$ by $\mathcal{A}_s$, the probability is easily obtained. □

Based on this probability, we can recalculate the coverage ratios in Eqn.(9), (10), (11), and (15).

In the deterministic deployment case, the proposed algorithms are effect for FoIs with holes. The only change is the input: partition $P = (S_i)$ involves only the effective area of the FoI not including the hole (e.g., the area of the grey part in Fig.3(b)).

2.2 Extend to Other Sensors

(i) *Sensors with heterogeneous sensing area.*

Only if the heterogeneous sensing area $\mathcal{A}_s$ can be modeled, i.e., A_s's area and perimeter can be formulated by mathematic function as $a(\mathcal{A}_s)$ and $c(\mathcal{A}_s)$ (e.g., the Quasi Model in [6]), our methods can still adopt to calculate the coverage ratio in stochastic distribution case. Replace πr^2 by $a(\mathcal{A}_s)$ and replace $2\pi r$ by $c(\mathcal{A}_s)$ in Eqn.(9), (10), (11), and (15), then the results in different distributions are obtained. Moreover, in the deterministic deployment case, our algorithms are also available due to the modeled sensing area.

(ii) *Mobile sensors.*

Using mobile sensors to improve the surface coverage ratio is an interesting problem. The surface solution by mobile sensors is significantly different from the static sensors. We leave it as our future work.

2.3 Extend to Arbitrary Distribution

We considered the *PP3* and *SP3* distribution before. We extend to arbitrary distribution $Y(\mathcal{A}_f)$, (e.g., the distribution of sensors may follow a zero-mean two-dimensional Gaussian distribution around the center of $\mathcal{A}_f$.) with probability density function $f(x, y)$ for coverage ratio computation in the deterministic deployment case. The following lemma is extended from [3].

Lemma S2.1. *Let FoI $\mathcal{A}_f$ be a convex area of area F_f and perimeter L_f. Let a certain sensor $\mathcal{A}_s$ be convex area of area F_s and perimeter L_s. Sensors are dropped on the FoI according to the distribution $Y(\mathcal{A}_f)$. The probability that a randomly selected point P in $\mathcal{A}_f$ is covered by $\mathcal{A}_s$ is given by*

$$p(P \in \mathcal{A}_s) = \frac{2\pi \int_{P \in \mathcal{A}_f} f(x,y)dx \wedge dy}{\int_{\mathcal{A}_f \cap \mathcal{A}_i \neq \emptyset} f(x,y)dx \wedge dy \wedge d\phi}. \quad (3)$$

With this Lemma, we can calculate the surface coverage ratio for any arbitrary distribution as long as the distribution of sensors is known.

2.4 Extend to Other Coverage Requirement

(i) *The requirement of k-coverage*

We considered the expected coverage ratio for full coverage. i.e., any point of FoI is at least covered by one sensor, which we also call 1-coverage. Our method also can be extended to calculate the coverage ratio for k-coverage that any point of FoI is at least covered by k sensors. The following lemma is derived from Eqn.(4).

Lemma S2.2. *Let N sensors be randomly and independently deployed on a FoI $\mathcal{A}_f$ of area F_f and perimeter L_f. Let a sensor A_s be a convex area of area F_s and perimeter L_s. The probability $p(\beta(P) = k)$ that a randomly selected point $P \in \mathcal{A}_f$ is covered by exactly k sensors is given by*

$$p(\beta(P) = k) \begin{cases} \prod_{s=1}^{N} \left(\frac{2\pi F_f + L_f L_s}{2\pi(F_f + F_s) + L_f L_s} \right), & k = 0, \\ \frac{\sum_{s=1}^{\binom{N}{k}} \left(\prod_{j=1}^{k} 2\pi F_{T(s,j)} \prod_{z=1}^{N-k} (2\pi F_f + L_f L_{G(s,z)}) \right)}{\prod_{r=1}^{N} (2\pi(F_f + F_r) + L_f L_r)}, & k \geq 1. \end{cases}$$

where T is a matrix. Each row j of T is a "k-choice" of $[1...N]$ (i.e., a vector with k elements out of N). And G is another matrix. Each row j of G contains the elements that do not appear in the j-th row of T.

The detailed proof of this lemma can refer to [5], [3]. Then, the expected coverage ratio for k-coverage is:

$$E(f_c) = p(\beta(P) \geq k) = \begin{cases} 1, & k = 0, \\ 1 - \sum_{l=0}^{k-1} \frac{\sum_{s=1}^{\binom{N}{k}} \left(\prod_{j=1}^{k} 2\pi F_{T(s,j)} \prod_{z=1}^{N-k} (2\pi F_f + L_f L_{G(s,z)}) \right)}{\prod_{r=1}^{N} (2\pi(F_f + F_r) + L_f L_r)}, & k \geq 1. \end{cases}$$

In the deterministic deployment case, it is easy to extend that deploys k sensors at every position obtained by our algorithms. Consequently, the k-coverage is achieved and it costs totally k times sensors compared with the full coverage requirement.

(ii) *The requirement of connectivity.*

If $\frac{r_c}{r_s} \geq 2$, the full coverage has satisfied the limitation of connectivity [7], where r_c is the communication range and r_s is the sensing range of a sensor. If $\frac{r_c}{r_s} \leq 2$ and the FoI is an ideal plane, existing research [1] proposes several deployment patterns to solve the connectivity and coverage problem. But if $\frac{r_c}{r_s} \leq 2$ and the FoI is a complex surface, the requirement of connectivity remains an open problem.

REFERENCES

[1] X. Bai, D. Xuan, Z. Yun, T. H. Lai, and W. Jia. Complete optimal deployment patterns for full-coverage and k-connectivity (k≤6) wireless sensor networks. In *ACM MobiHoc*, pages 401–410, New York, NY, USA, 2008.

[2] D. S. Hochbaum and W. Maass. Approximation schemes for covering and packing problems in image processing and vlsi. *J. ACM*, 32(1):130–136, 1985.

[3] L. Lazos and R. Poovendran. Stochastic coverage in heterogeneous sensor networks. *ACM Trans. Sen. Netw.*, 2(3):325–358, 2006.

[4] D. Lichtenstein. Planar formulae and their uses. *SIAM Journal on Computing*, 11(2):329–343, 1982.

[5] L. A. SANTALO. *Integral geometry and geometric probability*. Addison-Wesley, Massachusetts (etc.), 1976.

[6] S. Schmid and R. Wattenhofer. Algorithmic models for sensor networks. In *IEEE IPDPS*, pages 11–pp, 2006.

[7] H. Zhang and J. Hou. Maintaining sensing coverage and connectivity in large sensor networks. *Ad Hoc & Sensor Wireless Networks*, 1(1-2), 2005.